

Supporting Information

Dual-functional Bi-doped Co₃O₄ Nanosheets Array Towards High Efficiency 5-Hydroxymethylfurfural Oxidation and Hydrogen Production

Tianran Wei et al.

Experimental section

Synthesis

In the first step, a 1*2 cm² piece of nickel foam was cut out, then washed with dilute hydrochloric acid, anhydrous ethanol, acetone and methanol for 5 minutes respectively in order to remove the oxidized layer on the surface as well as the residual organic substance, and finally soaked in methanol and set aside; in the second step, Co(NO₃)₂·6H₂O 1.02g, Bi(NO₃)₃·5H₂O 0.243g, dissolved together in 15 ml of methanol, stirred to form solution A, and then weighed 2-Methylimidazole 0.616 mg, dissolved in 15 ml of methanol, stirred to form solution B. The solution A and solution B were mixed well and poured into 50 ml of reaction vessel liner, and then the treated nickel foam was inserted vertically into it, and the hydrothermal reaction was carried out at 120 °C for 4 hours. The thermal reaction was prepared to obtain BiCo-MOF precursor, which was naturally cooled to room temperature, rinsed the precursor with methanol three times, and dried in a vacuum oven at 60 °C for 6 h; in the third step, the precursor was placed in a quartz tube furnace and calcined at 350 °C for 2 h in air (the heating rate was 10 °C/min), and finally BiCoO-NA/NF was obtained. For comparison, the CoO-NA/NF sample was prepared under the identical process but without Bi doping.

Material characterizations

The apparent morphology and structure of the materials were characterized using a field emission scanning electron- microscope (SEM) (Nova NanoSEM 450, PNAlytical, Netherlands) and a transmission electron microscope (TEM) (Tecnai G2 F30 STwin, Philips-FEI, Netherlands). The crystal structure of the materials was characterized using an X-ray diffractometer (XRD) (X'Pert PRO type, PNAlytical, Netherlands) in the range of 5° to 80°. Using an x-ray photoelectron spectrometer (XPS) (Thermo Scientific K-Alpha, Shimadzu Kratos) to characterize the surface chemistry of the material (using Al (Ka) radiation as a probe). The binding energy was calibrated using the carbon peak (C 1s: 284.8 eV). The chemical structure of the material was tested and analyzed using a Raman spectrometer (LabRAM HR800, Horiba Jobin Yvon, France).

Electrochemical tests

The electrochemical tests were all performed on a CHI760e electrochemical workstation. The catalytic performances of the catalysts were tested with a three-electrode system, in which the studied sample, carbon rod and saturated Hg/HgO were used as working, counter and reference electrode, respectively. The linear scanning voltammetry (LSV) polarization curves were obtained at a slow sweep rate of 5 mV s⁻¹ under 1M KOH/1M KOH+0.5 M HMF. EIS was tested at open circuit voltage and in the frequency range of 0.1 to 100000 Hz. The electrical double layer capacitance (C_{dl}) was calculated

from cyclic voltammograms (CV) obtained in the non-Faraday interval (5 ~ 25 mV s⁻¹) and used to evaluate the electrochemically active specific surface area (ECSA).

The concentration variations of HMF and its oxidation products during the electrolysis were monitored through high-performance liquid chromatography (HPLC, Shimadzu Prominence LC-20AD) on aliquots taken from the electrochemical cells with an ultraviolet-visible detector. 20 µL of electrolyte was sampling during potentiostatic electrolysis and diluted to 2 mL with ultrapure water and analyzing it by HPLC. The wavelength of the UV detector was set to 265 nm, mobile phase A and phase B was methanol and 5 mmol L⁻¹ ammonium formate aqueous solution, respectively. The ratio of A: B was 3:7 and flow rate was 0.6 mL min⁻¹. A 4.6 mm 250 mm Ultimate 5 µm AQ-C18 column was used and each separation lasts 10 min.

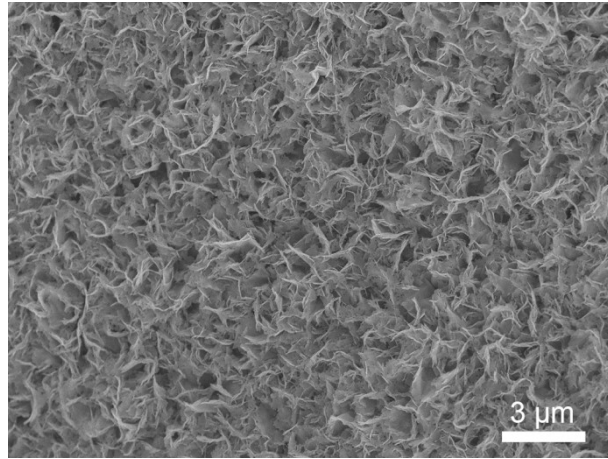


Figure S1. SEM image of BiCo-MOF/NF.

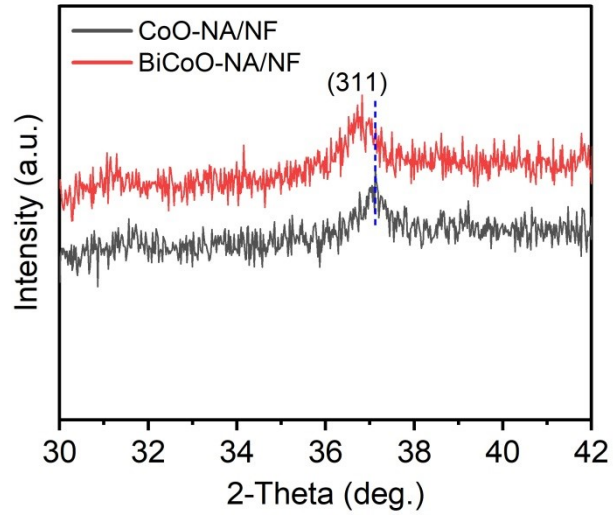


Figure S2. The enlarged XRD pattern of BiCo-MOF/NF. The ion radius of Bi^{3+} (1.03 Å) is larger than that of Co^{2+} (0.74 Å) and Co^{3+} (0.63 Å), resulting in the band length of Bi-O being longer than that of Co-O, and then the lattice constant of Co_3O_4 was increased.

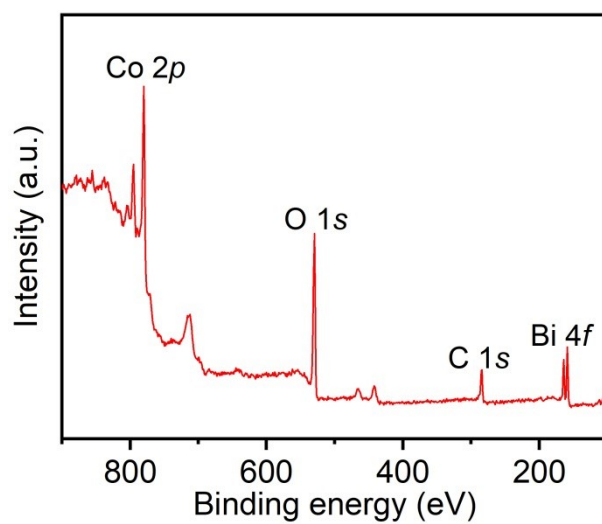


Figure S3. XPS survey spectra of BiCoO-NA/NF.

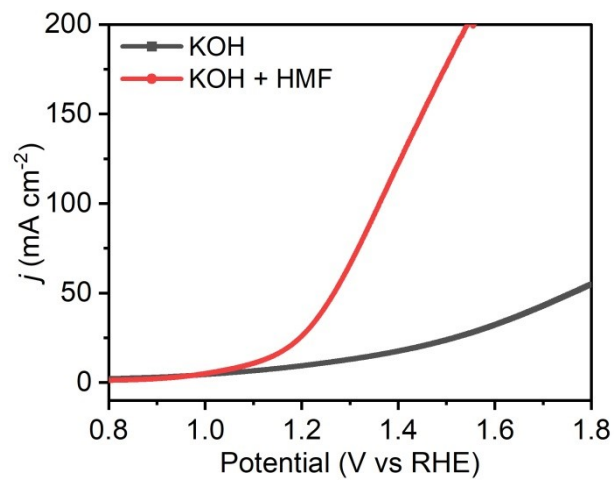


Figure S4. LSV curves of BiCoO-NA/NF recorded in different electrolytes.

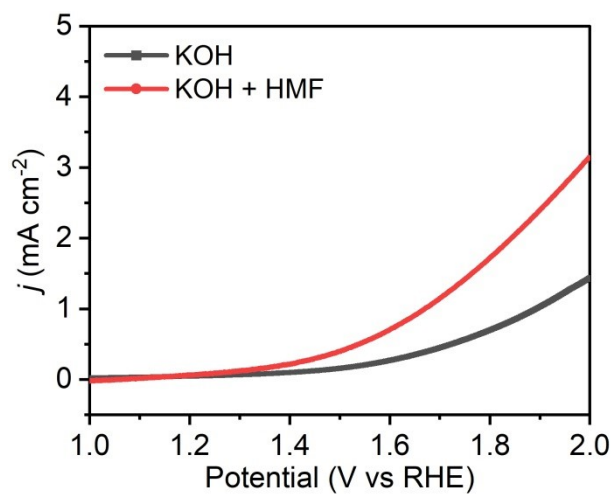


Figure S5. LSV curves of pure NF recorded in different electrolytes.

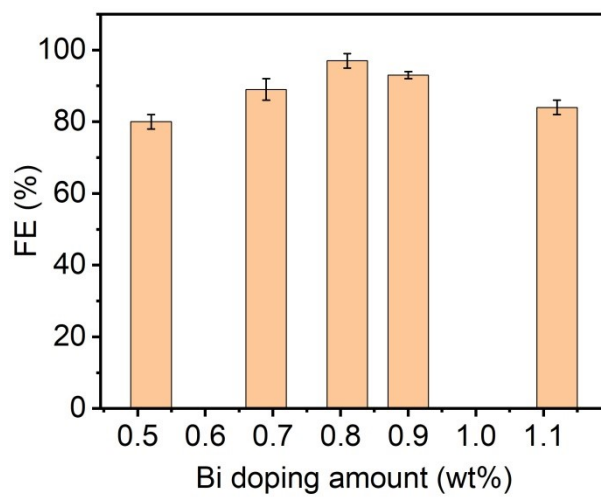


Figure S6. The effect of Bi doping amount in BiCoO-NA/NF on HMF oxidation.

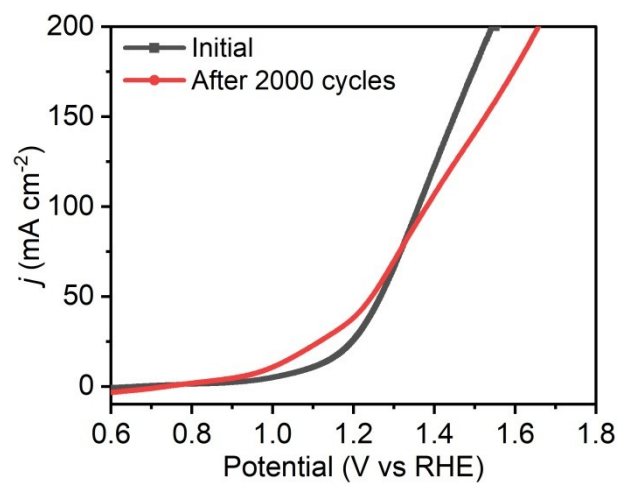


Figure S7. LSV curves of BiCoO-NA/NF recorded before and after 2000 cycles.

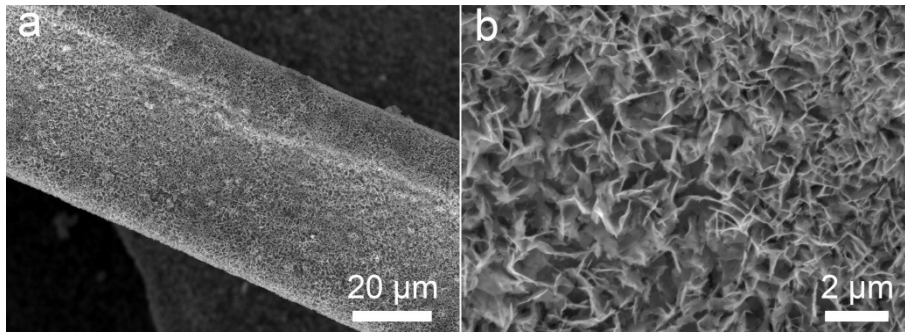


Figure S8. SEM image of BiCoO-NANF after the electrolysis.

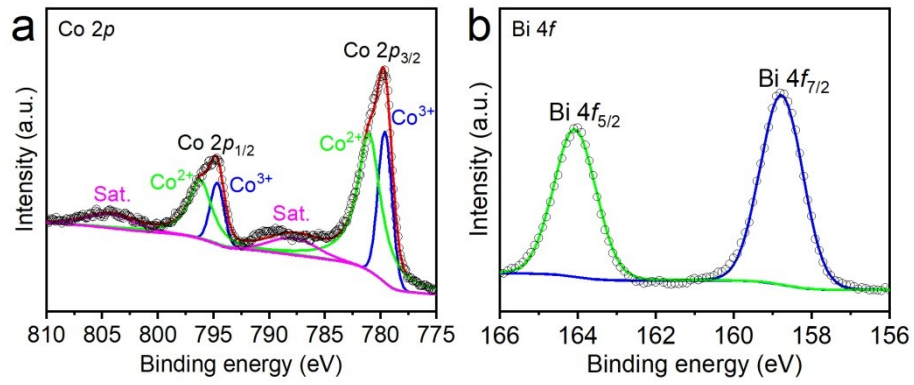


Figure S9. High resolution Co 2p and Bi 4f XPS spectra for BiCoO-NA/NF after the electrolysis.

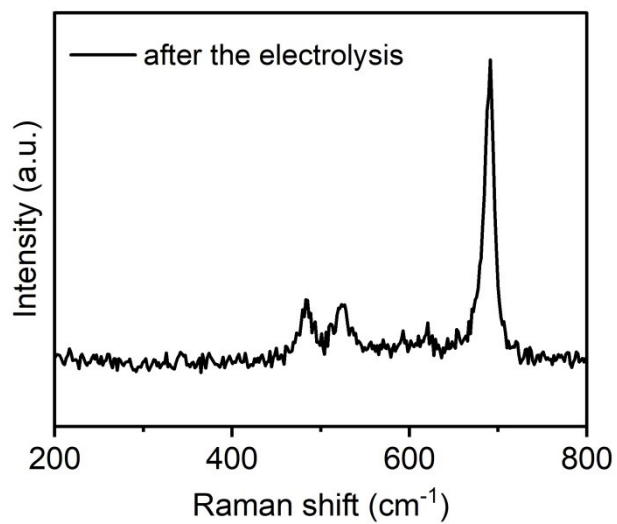


Figure S10. Raman spectrum for BiCoO-NA/NF after the electrolysis.

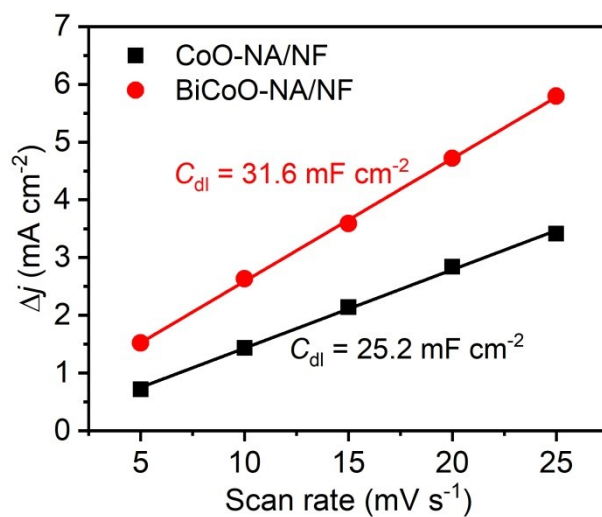


Figure S11. Capacitive currents depending on scan rates of CoO-NA/NF and BiCoO-NA/NF.

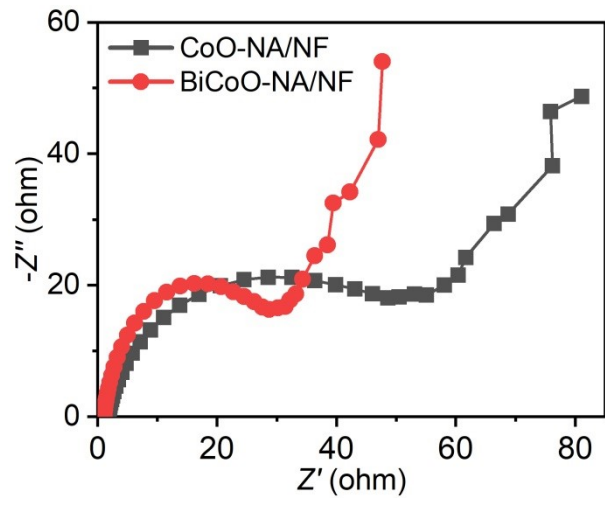


Figure S12. Nyquist plots of CoO-NA/NF and BiCoO-NA/NF.

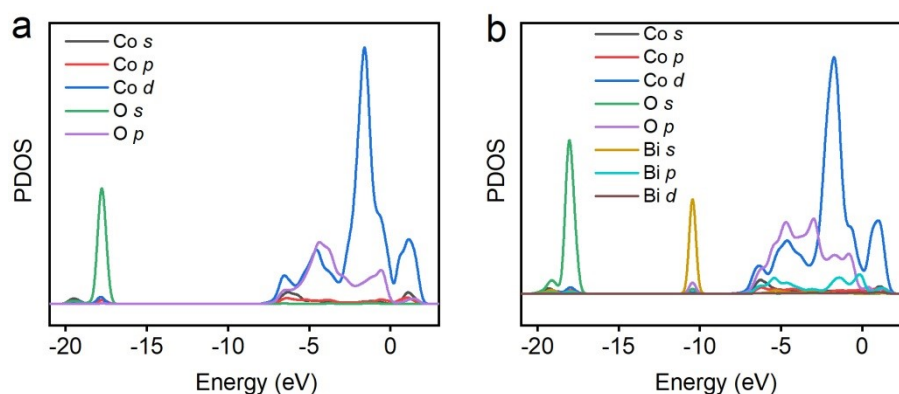


Figure S13. The calculated PDOS for CoO-NA/NF and BiCoO-NA/NF. As seen, the orbitals of Bi are hybridized with Co and O orbitals to yield new impurity energy level, which indicates that Bi attracts electrons from adjacent Co atom. This electron transfer is also reflected in the Co 2*p* XPS analyses (Figure 2b), which showed that a positive shift is observed after Bi doping. Also, the incorporation of Bi dopant induces a better conductivity and thereby accelerating the charge transfer during the electrolysis (refs. 24 and 25), which has been confirmed by the Nyquist plots (Figure S12). Meantime, we also calculated the HMF adsorption energy (ΔE_{HMF}) on CoO-NA/NF and BiCoO-NA/NF (Figure S14), which demonstrated that BiCoO-NA/NF shows a ΔE_{HMF} of -1.31 eV, smaller than that of CoO-NA/NF ($\Delta E_{\text{HMF}} = -1.02$ eV), suggesting that the Bi dopant could promote the HMF adsorption. The above results collectively indicates that Bi dopant significantly engineers the electronic structure of Co_3O_4 , which induces more active sites and promotes charge transfer, accompanied by the reactants affinity.

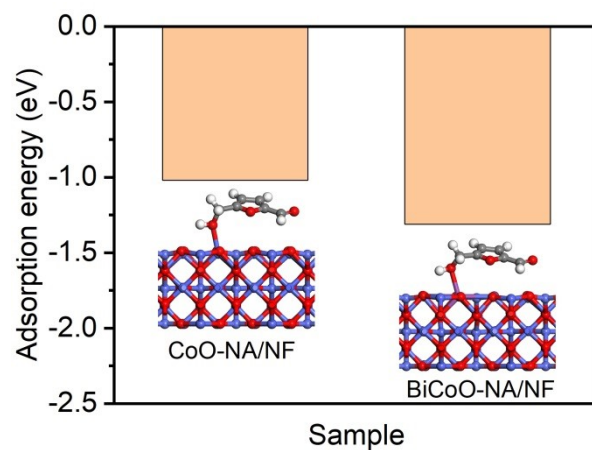


Figure S14. The calculated HMF adsorption energy for CoO-NA/NF and BiCoO-NA/NF.

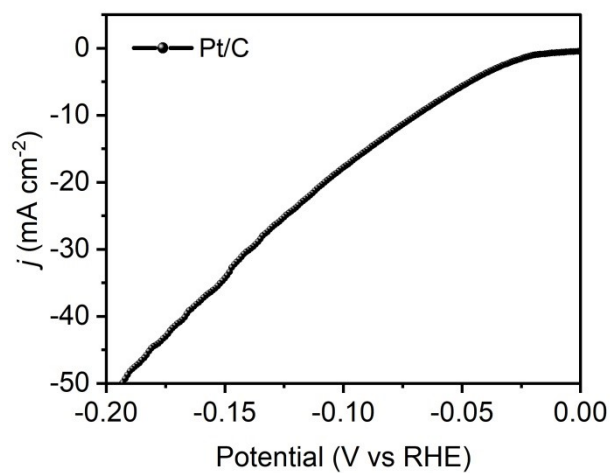


Figure S15. The HER LSV curve of 20 wt% Pt/C tested in alkaline electrolyte.

As seen, the overpotential to reach -10 mA cm^{-2} is 70 mV, superior than that of BiCoO-NA/NF (125 mV).